

# Enhancing Security Measures: Leveraging Fuzzy Logic Integration for Prohibited Item Detection in Dual-Energy X-Ray Security Inspection

Ozan Yalçın<sup>a,b,\*</sup> and Mehmet Önder Efe<sup>b</sup>

<sup>a</sup>Roketsan Inc., Lalahan, Ankara, Turkey, 06852

<sup>b</sup>Hacettepe University, Department of Computer Engineering, Beytepe, Ankara, Turkey, 06800

## ABSTRACT

This study aims to develop a threat detection algorithm strengthened by fuzzy logic for Dual-Energy X-Ray Security systems. Fuzzy-Logic Integrated Threat Detection (FLITD) allows for the handling of uncertainties and imprecise information often encountered in real-time baggage scanning processes, and the separation of threatening and non-threatening items although many of the features are similar. In contrast to conventional methods traditional, by leveraging fuzzy sets and membership functions, the system evaluates ambiguous or borderline threat indicators, such as densities and material compositions. Thus, it rigorously quantifies the associated threat probabilities. This approach enables a more flexible decision-making process, reducing error rates and improving detection performance. Experimental results demonstrate that the Fuzzy-Logic Integrated Threat Detection algorithm significantly outperforms conventional systems in both detection and accuracy.

**Keywords:** Fuzzy Logic, Threat Detection, X-Ray Imaging, Dual-Energy X-Ray, Effective Atomic Number, Explosive Detection

## 1. INTRODUCTION

Nowadays, X-Ray technologies are used in a wide range of fields, such as healthcare and security. In the field of security, X-Ray baggage inspection systems (XBIS) play a critical role in protecting people from threats and attacks by screening packages. Furthermore, the automatic detection and screening capabilities of XBIS improve as a result of novel studies conducted by researchers and technologists.<sup>1</sup> Thus, places will become safer for people through the use of various types of XBIS, such as single-view (SV), dual-view (DV) and Computed Tomography (CT), in areas such as shopping centers, subways and especially airports.<sup>2</sup>

As is well-known, the identification of the materials inside a package is the main process for XBIS. Estimation of the effective atomic number ( $Z_{eff}$ ) is the most powerful and widely used method for identifying materials, as  $Z_{eff}$  serves as a descriptor for compounds.<sup>3</sup> To estimate  $Z_{eff}$ , the mass attenuation coefficients ( $\mu$ ) and the ratio ( $R$ ) of the mass attenuation coefficients for high energy (HE) and low energy (LE) data have been used in numerous studies.<sup>4,5</sup> The relation between  $\mu_{HE}$ ,  $\mu_{LE}$ , and ( $R$ ) can be expressed as shown in (1).<sup>6</sup> In addition,  $Z_{eff}$  for a compound can be easily calculated using the formula given in (2).<sup>7</sup>

$$\mu_{HE} = \frac{-\ln(\frac{I_{HE}}{I_0})}{x}, \quad \mu_{LE} = \frac{-\ln(\frac{I_{LE}}{I_0})}{x} \quad \text{and then} \quad R = \frac{\mu_{HE}}{\mu_{LE}} \quad (1)$$

$$Z_{eff} = \sqrt[2.94]{\sum \alpha_i Z_i^{2.94}} \quad \text{where} \quad \alpha_i = \frac{n_i Z_i}{\sum n_i Z_i} \quad (2)$$

As seen in Fig. 1.1, after generating the ratio  $R$ , it can be converted to  $Z_{eff}$  for each pixel in the HE and LE raw images, based on the characteristic equations of the system.

---

Further author information: (Send correspondence to Ozan Yalçın)  
Ozan Yalçın: E-mail: yalcinozn@gmail.com

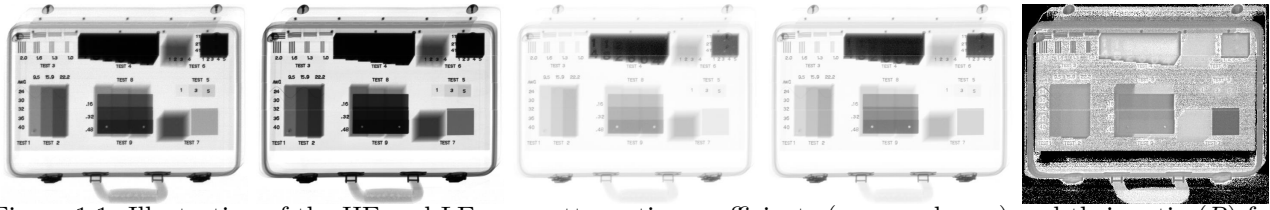


Figure 1.1: Illustration of the HE and LE mass attenuation coefficients ( $\mu_{HE}$  and  $\mu_{LE}$ ) and their ratio ( $R$ ) for various materials, obtained using the ASTM F792-08 test kit.

The  $Z_{eff}$  model can serve as the basis for both material classification and detection within XBIS. By utilizing this model, materials can be classified as organic, inorganic, or metal, aiding the identification process and improving the accuracy of security screenings.<sup>8</sup> Beyond classification, the detection of explosives<sup>6</sup> and drugs<sup>9</sup> is possible with the aid of the  $Z_{eff}$  model. Its ability to recognize specific characteristics of these materials allows for more precise identification, improving the effectiveness of XBIS in protecting public spaces, and increasing security measures.

Numerous studies have focused on improving the detection capabilities of X-Ray Baggage Inspection Systems (XBIS). These studies have explored not only the  $Z_{eff}$  estimation models but also deep learning techniques,<sup>10-13</sup> which have gained significant attention for their potential to improve the identification of material and the detection of threats performance. In this study, the goal is to improve the detection capability while minimizing the high computational demands typically associated with deep learning models. To achieve this, a fuzzy logic-based approach has been developed. Fuzzy logic is a method of reasoning that allows for approximate rather than precise reasoning, making it suitable for handling uncertainty and imprecision. It is commonly used in control systems, decision making, and pattern recognition tasks, where traditional binary logic is not. In this work, fuzzy logic has been applied to develop the Fuzzy Logic Integrated Threat Detection (FLITD) model, which effectively distinguishes between hazardous and non-hazardous materials using features extracted from X-Ray data.

### 1.1 Problem Statement

In X-Ray security inspection systems, distinguishing between hazardous materials such as PETN, HMTD, ANFO, potassium perchlorate and nonhazardous materials such as water and salt presents a significant challenge. These materials share similar values in key parameters, such as effective atomic number ( $Z_{eff}$ ) and the ratio of mass attenuation coefficients ( $R$ ). As an illustration, PETN has a  $Z_{eff}$  value of 7.4, while water has a  $Z_{eff}$  value of 7.42. The overlap of these values makes it difficult to differentiate between these substances in X-Ray images, leading to potential classification errors.

Current methods, relying on traditional X-Ray image analysis and basic parameter comparisons, fall short in accurately distinguishing between materials with overlapping properties. Therefore, a more advanced approach capable of effectively differentiating between these materials and improving detection accuracy is needed.

### 1.2 Proposed Method

This study proposes a novel method, called Fuzzy Logic Integrated Threat Detection (FLITD), to address the challenge of similar or overlapping values of  $R$  and  $Z_{eff}$  for different materials. FLITD can distinguish between overlapping materials by examining HE, LE,  $\mu_{HE}$ ,  $\mu_{LE}$ ,  $R$ , and the differently weighted fused data from HE and LE. This method allows for the precise differentiation between PETN (7.4), a hazardous material, and water (7.42), a non-hazardous substance, despite their similar properties like  $R$  and  $Z_{eff}$ . All details of the methodology and our approach will be thoroughly explored in the following section.

## 2. METHODOLOGY

To thoroughly understand and analyze the overlapping problem, six non-hazardous materials and six explosive materials<sup>14</sup> were selected for this study. The  $R$  and  $Z_{eff}$  values of these materials, categorized as organic and inorganic, are presented in Table 1. As seen in Figure 2.1, the overlap between  $R$  and  $Z_{eff}$  values poses a critical

issue in security screening systems, as chemically distinct substances can appear similar in X-Ray images. As a result, this can cause false positives or false negatives, reducing the effectiveness of the system.

Table 1:  $R$  and  $Z_{eff}$  values for Sample Materials

No	Material	Code/Formula	$R_{measured}$	$Z_{eff}$	Category
1	Ammonium Nitrate	TSK-8010	0.834	6.9	Organic
2	Sucrose	$C_{12}H_{22}O_{11}$	0.841	6.92	Organic
3	HMTD	TSK-9060	0.835	7.0	Organic
4	Glucose Mono-hydrate	$C_6H_{12}O_6, H_2O$	0.838	7.0	Organic
5	ANFO	TSK-8020	0.827	7.1	Organic
6	PETN	TSK-9099	0.808	7.4	Organic
7	Water	$H_2O$	0.829	7.42	Organic
8	Potassium Perchlorate	TSK-1205	0.607	15.0	Inorganic
9	Calcium Carbonate	$CaCO_3$	0.599	15.08	Inorganic
10	Salt	$NaCl$	0.604	15.18	Inorganic
11	Termite	TSK-8060	0.573	21.2	Inorganic
12	Manganese Dioxide	$MnO_2$	0.565	21.29	Inorganic

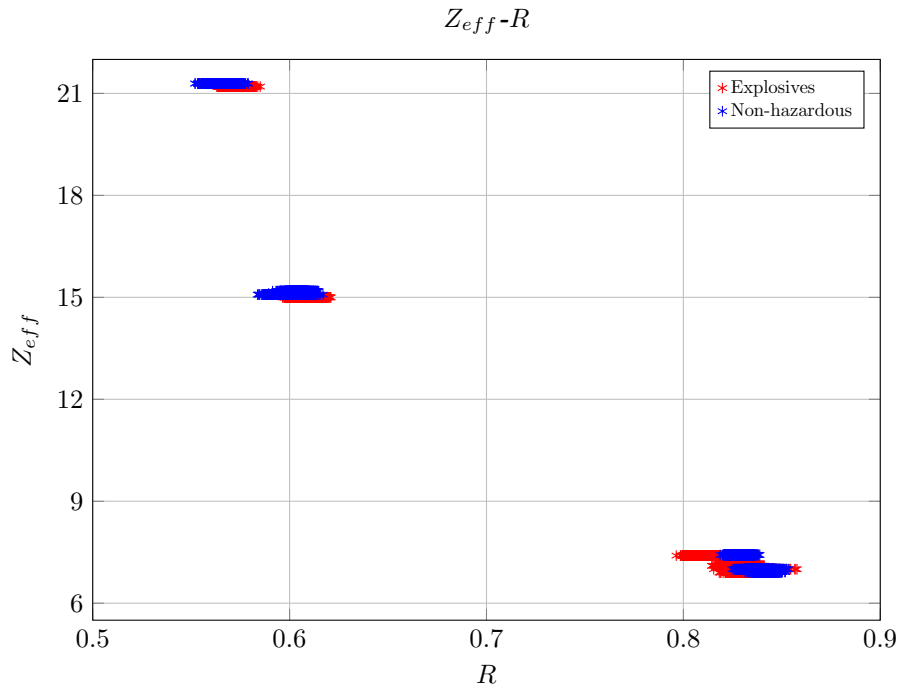


Figure 2.1: Illustration of the ratio ( $R$ ) and  $Z_{eff}$  for the sample materials.

In order to address the challenge of the overlapping problem, it becomes evident that relying solely on  $R$  is insufficient to distinguish all materials from one another. Therefore, additional material-specific information is required. Initially, only HE and LE raw data can be obtained from the X-Ray detectors; however, it is possible to derive further information by utilizing both HE and LE. For instance, the variables  $\mu_{HE}$  and  $\mu_{LE}$  are used to calculate  $R$ , as shown in (1), and both variables are derived directly from the HE and LE data. Consequently,  $\mu_{HE}$  and  $\mu_{LE}$  can serve as supplementary features along with  $R$ . Up to this point, five distinct pieces of information are available: HE, LE,  $\mu_{HE}$ ,  $\mu_{LE}$ , and  $R$ .

If further information is required, additional features, such as fused data, can be derived through advanced

processing of HE and LE raw data, potentially enhancing material differentiation capability. Fused data refers to the combination of HE and LE with varying weights. In this study, nine fused data are used from  $F_{19}$  to  $F_{91}$ , and the fused data are generated by using the expression in (3).

$$F_{ab} = \frac{a}{a+b} * HE + \frac{b}{a+b} * LE \quad \text{where } a + b = 10 \quad (3)$$

In this study, Adaptive Calibration is applied to all HE and LE raw images during pre-processing to eliminate noise and distortions. Afterward, a  $5 \times 5$  smoothing filter is applied to further refine the images. For the creation of dataset, nine hundred pixels ( $30 \times 30$ ) are sampled from each material listed in Table 1. From these sampled pixels, the features  $\mu_{HE}$ ,  $\mu_{LE}$ ,  $R$ ,  $F_{19}$ ,  $F_{28}$ ,  $F_{37}$ ,  $F_{46}$ ,  $F_{55}$ ,  $F_{64}$ ,  $F_{73}$ ,  $F_{82}$ , and  $F_{91}$  are derived. As a result, a dataset with nine hundred rows and fourteen columns is generated for each material. Additionally, 'threat information' is added as a binary column, labeled TRUE for hazardous materials and FALSE for non-hazardous materials, along with the  $Z_{eff}$  value. The structure of the resulting dataset is illustrated in Table 2. For the creation of the test set, similarly to the dataset, one hundred pixels ( $10 \times 10$ ) are sampled from the same materials listed in Table 1.

Table 2: Illustrative Sample from the Simplified Dataset

HE	LE	$\mu_{HE}$	$\mu_{LE}$	$R$	$F_{19}$	$F_{28}$	$F_{37}$	$F_{46}$	$F_{55}$	$F_{64}$	$F_{73}$	$F_{82}$	$F_{91}$	Decision	$Z_{eff}$
0.724	0.582	-0.322	-0.540	0.596	0.596	0.610	0.625	0.639	0.653	0.667	0.681	0.696	0.710	0	15.08
0.720	0.579	-0.327	-0.545	0.600	0.593	0.607	0.622	0.636	0.650	0.664	0.678	0.692	0.706	0	15.08
0.720	0.575	-0.327	-0.551	0.593	0.590	0.604	0.619	0.633	0.648	0.662	0.677	0.691	0.706	0	15.08
.	.	.	.	.	.	.	.	.	.	.	.	.	.	.	.
.	.	.	.	.	.	.	.	.	.	.	.	.	.	.	.
0.356	0.163	-1.032	-1.811	0.569	0.182	0.202	0.221	0.240	0.259	0.279	0.298	0.317	0.336	1	21.2
0.351	0.162	-1.035	-1.817	0.569	0.181	0.200	0.220	0.239	0.258	0.278	0.297	0.316	0.335	1	21.2
0.360	0.166	-1.019	-1.791	0.568	0.186	0.205	0.224	0.244	0.263	0.283	0.302	0.322	0.341	1	21.2
0.361	0.167	-1.017	-1.788	0.568	0.186	0.206	0.225	0.244	0.264	0.283	0.303	0.322	0.342	1	21.2
0.360	0.167	-1.019	-1.785	0.569	0.186	0.205	0.225	0.244	0.263	0.283	0.302	0.322	0.341	1	21.2
.	.	.	.	.	.	.	.	.	.	.	.	.	.	.	.
.	.	.	.	.	.	.	.	.	.	.	.	.	.	.	.
0.570	0.508	-0.560	-0.675	0.829	0.515	0.521	0.527	0.533	0.539	0.546	0.552	0.558	0.564	1	7.1
0.568	0.506	-0.564	-0.679	0.830	0.512	0.519	0.525	0.531	0.537	0.543	0.549	0.556	0.562	1	7.1
0.568	0.505	-0.565	-0.682	0.829	0.511	0.518	0.524	0.530	0.536	0.543	0.549	0.555	0.561	1	7.1
0.567	0.504	-0.566	-0.683	0.828	0.511	0.517	0.523	0.530	0.536	0.542	0.548	0.555	0.561	1	7.1
0.570	0.506	-0.561	-0.679	0.826	0.513	0.519	0.525	0.532	0.538	0.544	0.551	0.557	0.563	1	7.1
0.573	0.508	-0.556	-0.675	0.823	0.515	0.521	0.528	0.534	0.541	0.547	0.554	0.560	0.566	1	7.1
0.571	0.508	-0.559	-0.676	0.828	0.514	0.521	0.527	0.533	0.539	0.546	0.552	0.558	0.564	1	7.1

## 2.1 Designing Fuzzy Logic

After the dataset is generated, the design of the fuzzy logic system for hazardous material detection is carried out using MATLAB, along with the Fuzzy Logic Toolbox and the Image Processing Toolbox. In this study, FLITD has  $n$  inputs and a single output, which is either TRUE or FALSE. As mentioned before, the feature  $R$  is not enough to distinguish explosives from non-hazardous materials; however, using all features derived from HE and LE in Table 2 may not be mandatory. To determine the essential features, several experiments were conducted and the results are compared.

In this study, Sugeno-Type Fuzzy Logic was preferred to develop FLITD. In the Sugeno-type fuzzy inference system, the output is a weighted sum of the input variables, making it suitable for function approximation and control applications. A typical first-order Sugeno fuzzy model consists of rules in the form as given (4), (5) and (6).<sup>15</sup> This formulation ensures a smooth and computationally efficient inference mechanism, making Sugeno-type fuzzy logic particularly advantageous for real-time decision-making applications.

$$y^i = p_1^i x_1 + p_2^i x_2 + \dots + p_n^i x_n + q^i \quad (4)$$

$$y = \frac{\sum_{i=1}^M w^i y^i}{\sum_{i=1}^M w^i} \quad (5)$$

$$w^i = \mu_{A_1^i}(x_1) \cdot \mu_{A_2^i}(x_2) \dots \mu_{A_n^i}(x_n) \quad (6)$$

Where:

- $x_1, x_2, \dots, x_n$  are input variables,
- $A_1^i, A_2^i, \dots, A_n^i$  are fuzzy sets associated with the inputs,
- $p_1^i, p_2^i, \dots, p_n^i$  and  $q^i$  are linear coefficients that define the rule output  $y^i$ ,
- $i$  denotes the rule index,
- $w^i$  is the firing strength of the  $i^{th}$  rule,
- $M$  is the total number of fuzzy rules.

MATLAB Fuzzy Logic Toolbox was utilized to analyze inputs and outputs for fuzzy logic modeling. FLITD generates an output for each input set, providing a real number that indicates the probability of similarity to hazardous materials. An illustration of FLITD is presented in Figure 2.2. In this setup, there are fourteen inputs and a single output. The FLITD uses nine rules to investigate the output, with the number of rules varying based on the number of inputs, outputs, and the complexity of the problem.

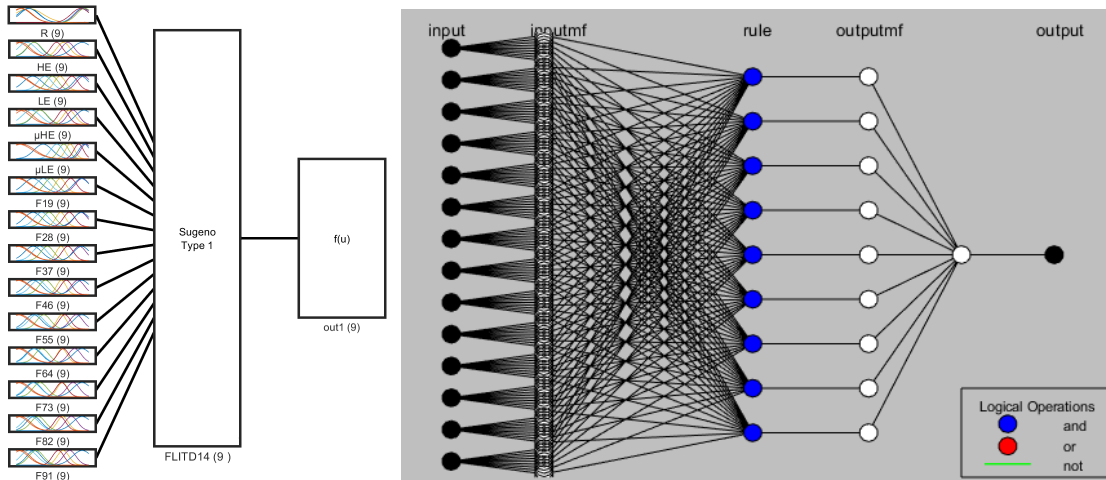


Figure 2.2: FLITD structure with fourteen inputs and a single output

In the next section, the tests conducted to create the most optimal and high-performing FLITD, along with the results obtained, are detailed.

### 3. TEST AND RESULT

In the development step of FLITD, the performance is analyzed by varying the number of input features ( $n$ ). To evaluate the performance, the following parameters are used: TP (True Positive), FP (False Positive), TN (True Negative), FN (False Negative), Precision, Recall, F1-Score, Accuracy and Specificity. To classify the materials as TRUE (hazardous) or FALSE (non-hazardous), a critical boundary is set at  $C_b = 0.5$ . If the output is smaller than 0.5, the material is classified as FALSE (non-hazardous), whereas if the output exceeds 0.5, it is classified as TRUE (hazardous).

Table 3: Performance metrics of FLITD with varying numbers of input features.

No	Input Features	Rules	Process Time	TP	FP	TN	FN	Precision	Recall	F1-Score	Accuracy	Specificity
1	R	4	1T	100	75	75	50	0.571	0.667	0.615	0.583	0.500
2	R, HE	4	1.15T	125	75	75	25	0.625	0.833	0.714	0.667	0.500
3	R, HE, LE	4	1.44T	129	100	50	21	0.563	0.860	0.681	0.597	0.333
4	R, HE, LE, $\mu$ HE	7	2.00T	100	100	50	50	0.500	0.667	0.571	0.500	0.333
5	R, HE, LE, $\mu$ HE, $\mu$ LE	7	2.05T	150	25	125	0	0.857	1.000	0.923	0.917	0.833
6	R, HE, LE, $\mu$ HE, $\mu$ LE, F19	7	2.19T	150	25	125	0	0.857	1.000	0.923	0.917	0.833
7	R, HE, LE, $\mu$ HE, $\mu$ LE, F19, F28	8	2.71T	150	25	125	0	0.857	1.000	0.923	0.917	0.833
8	R, HE, LE, $\mu$ HE, $\mu$ LE, F19 to F37	8	2.78T	150	25	125	0	0.857	1.000	0.923	0.917	0.833
9	R, HE, LE, $\mu$ HE, $\mu$ LE, F19 to F46	8	3.18T	150	25	125	0	0.857	1.000	0.923	0.917	0.833
10	R, HE, LE, $\mu$ HE, $\mu$ LE, F19 to F55	9	4.19T	150	25	125	0	0.857	1.000	0.923	0.917	0.833
11	R, HE, LE, $\mu$ HE, $\mu$ LE, F19 to F64	9	4.29T	150	25	125	0	0.857	1.000	0.923	0.917	0.833
12	R, HE, LE, $\mu$ HE, $\mu$ LE, F19 to F73	9	4.54T	150	25	125	0	0.857	1.000	0.923	0.917	0.833
13	R, HE, LE, $\mu$ HE, $\mu$ LE, F19 to F82	9	4.76T	150	25	125	0	0.857	1.000	0.923	0.917	0.833
14	R, HE, LE, $\mu$ HE, $\mu$ LE, F19 to F91	9	5.03T	150	25	125	0	0.857	1.000	0.923	0.917	0.833

As presented in Table 3, the five-input model is determined to be the optimal choice for FLITD. Although increasing the number of features from five to fourteen does not improve performance, it significantly increases decision processing time, which is undesirable.

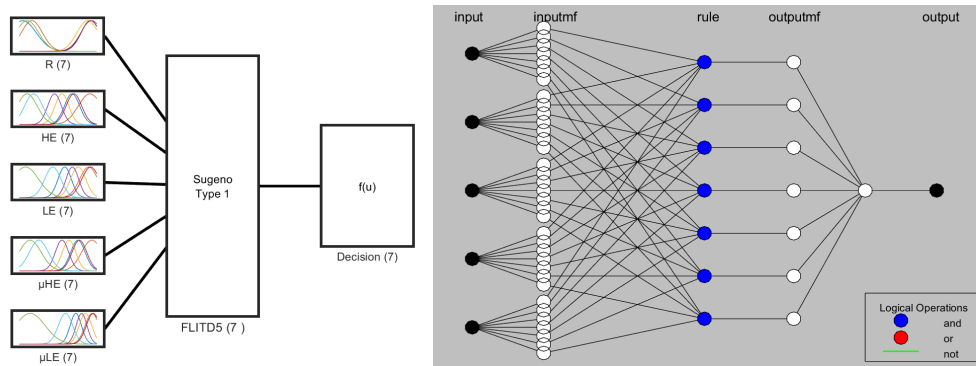


Figure 3.1: FLITD-5 structure with five inputs and a single output

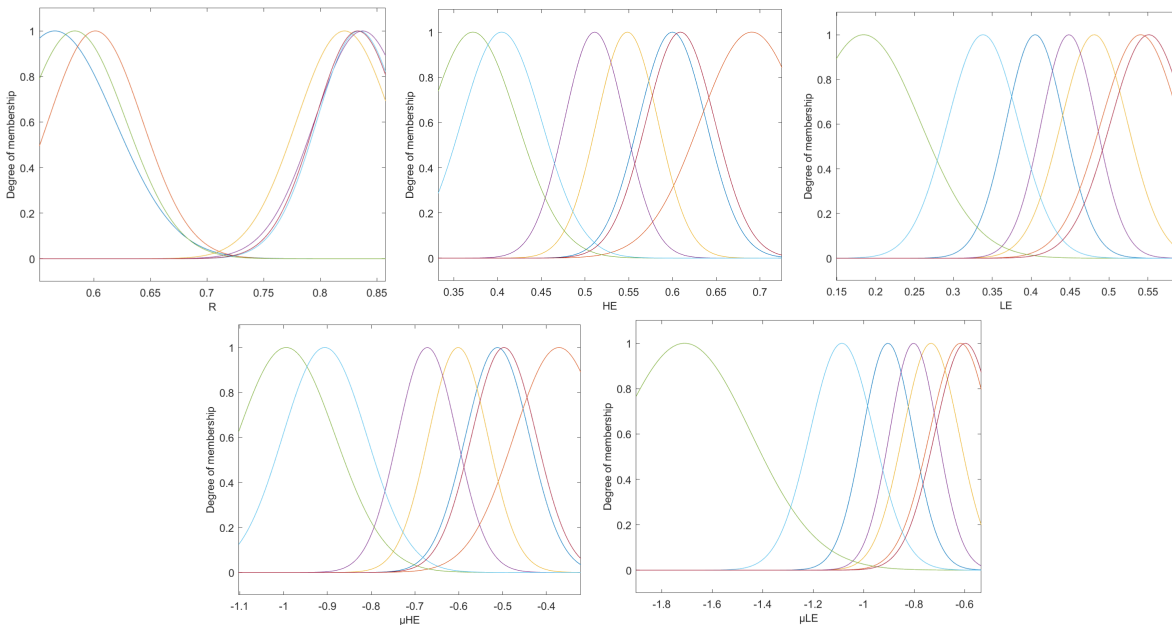


Figure 3.2: FLITD-5 structure with five inputs and a single output

All specifications of the FLITD-5, including the structure and operational parameters, are presented in Figure 3.1. Furthermore, the membership functions of the input features, which define the relationship between input values and fuzzy sets, are shown in detail in Figure 3.2. These membership functions play a crucial role in determining the degree of similarity to hazardous materials and enhancing the detection capability of the model.

As seen in Figure 3.3, the FLITD-5 model performs well in detecting explosives in sample cases. The evaluation results, presented in Table 3, provide a detailed comparison of different input configurations and their impact on performance metrics. Additionally, visual examples illustrate how the model distinguishes hazardous materials in various scenarios, demonstrating the role of selected features in the decision process.

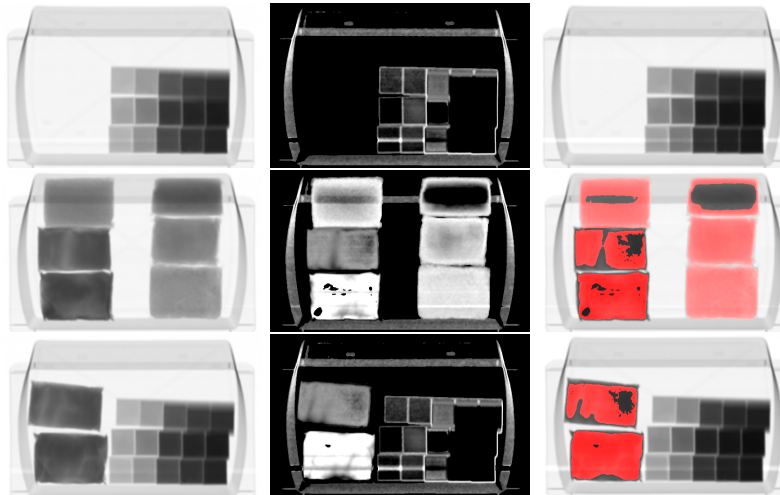


Figure 3.3: Visualization of hazardous material detection in X-Ray images using the FLITD-5 model.

#### 4. CONCLUSION AND DISCUSSION

In this study, a novel fuzzy logic-based method called FLITD (Fuzzy Logic Integrated Threat Detection) was developed to enhance the detection of hazardous materials in X-Ray images. The method aims to overcome the limitations of traditional detection models that rely solely on  $R$  and  $Z_{eff}$  values by incorporating additional features derived from High Energy (HE) and Low Energy (LE) data. This approach allows for better differentiation between hazardous and non-hazardous materials, addressing the challenge of overlapping values in material properties. The proposed FLITD model uses a set of input features, including  $R$ , HE, LE,  $\mu_{HE}$ , and  $\mu_{LE}$ , to improve the accuracy of hazardous material detection. Furthermore, FLITD maintains computational efficiency, allowing it to operate without the high processing demands typically associated with deep learning models.

Fuzzy logic has provided significant advantages in improving the detection of hazardous materials in X-ray images. It has allowed for better management of the inherent uncertainties in material properties, which is often a limitation in traditional methods. Unlike traditional approaches that rely on rigid thresholds, fuzzy logic evaluates probabilities, reducing the number of misclassifications, especially in cases where material properties overlap. Furthermore, the FLITD model, which uses fuzzy logic, achieved accuracy levels comparable to deep learning models while maintaining lower computational costs. This characteristic makes it more suitable for real-time applications, where processing speed is crucial. In summary, fuzzy logic has enabled improved detection accuracy, optimized processing time, and a more computationally efficient approach to hazardous material detection. Thus, FLITD offers a practical and effective alternative for security systems, combining high performance with minimal resource requirements.

The performance of the FLITD model was evaluated through various tests, and it was found that a five-input feature set offered the optimal balance between detection accuracy and computational efficiency. The results, presented in terms of TP (True Positive), FP (False Positive), TN (True Negative), FN (False Negative), Precision, Recall, F1-Score, Accuracy, and Specificity, demonstrate that FLITD outperforms other models with higher input features, which did not yield significant improvements and led to increased processing time. The

FLITD-5 model, with its optimized input set, showed promising results in detecting hazardous materials such as explosives, while maintaining low processing time.

For future work, the FLITD model can be further enhanced by expanding the dataset to include a larger variety of hazardous and non-hazardous materials. Increasing the number of data points would strengthen the model's detection capabilities. Additionally, further validation and testing with diverse datasets would help assess the robustness and scalability of model, making it more effective for use in security systems. Another area for improvement is reducing processing time, which can be achieved through techniques such as utilizing GPU, allowing for faster processing for detection of hazardous materials. This would make FLITD more suitable for real-time applications. Furthermore, exploring the deployment of FLITD in real-world security scenarios could provide valuable insights into its performance under different operational conditions.

## REFERENCES

- [1] Çiğla, C., Küçükateş, B., Yalçın, O., Ak, D. S., and Şükrücan Taylan Işıkoğlu, "Robust material classification on dual-energy x-ray imaging devices," in [*Anomaly Detection and Imaging with X-Rays (ADIX) VII*], **12104**, 1210404, SPIE (2022).
- [2] Khan, S., Khan, I., Ullah, I., Naveed, S., and Ullah, I., "A review of airport dual energy x-ray baggage inspection techniques: Image enhancement and noise reduction," *Journal of X-Ray Science and Technology* **28**, 1–25 (2020).
- [3] Kimoto, N., Hayashi, H., Asakawa, T., Lee, C., Asahara, T., Maeda, T., Goto, S., Kanazawa, Y., Katsumata, A., Yamamoto, S., and Okada, M., "Effective atomic number image determination with an energy-resolving photon-counting detector using polychromatic x-ray attenuation by correcting for the beam hardening effect and detector response," *Applied Radiation and Isotopes* **170**, 109617 (2021).
- [4] Chang, C.-H., Yu, N.-C., and Tseng, S.-P., "Calculation of effective atomic numbers using a rational polynomial approximation method with a dual-energy x-ray imaging system," *Journal of X-Ray Science and Technology* **29**, 1–14 (2021).
- [5] Kayalvizhi, R., Amit kumar, Malarvizhi, S., Topkar, A., and Vijayakumar, P., "Raw data processing techniques for material classification of objects in dual energy x-ray baggage inspection systems," *Radiation Physics and Chemistry* **193**, 109512 (2022).
- [6] Yalçın, O. and İskender Atilla Reyhancan, "Detection of explosive materials in dual-energy x-ray security systems," *Nuclear Instruments and Methods in Physics Research Section A: Accelerators, Spectrometers, Detectors and Associated Equipment* **1040**, 167265 (2022).
- [7] Bonnin, A., Duvauchelle, P., Kaftandjian, V., and Ponard, P., "Concept of effective atomic number and effective mass density in dual-energy x-ray computed tomography," *Nuclear Instruments and Methods in Physics Research Section B: Beam Interactions with Materials and Atoms* **318**, 223–231 (2014).
- [8] Benedykciuk, E., Denkowski, M., and Dmitruk, K., "Material classification in x-ray images based on multi-scale cnn," *Signal, Image and Video Processing* **15**, 1–9 (2021).
- [9] Vogel, H., Haller, D., Laitenberger, C., Heinemann, A., and Püschel, K., "Detection of drug transport using x-ray techniques," *Archiv für Kriminologie* **218**, 1–21 (2006).
- [10] Pourghassem, H., Sharifi-Tehrani, O., and Nejati, M., "A novel weapon detection algorithm in x-ray dual-energy images based on connected component analysis and shape features," *Australian Journal of Basic and Applied Sciences* **5**, 300–307 (2011).
- [11] Wei, Y., Zhu, Z., Yu, H., and Zhang, W., "Aftd-net: real-time anchor-free detection network of threat objects for x-ray baggage screening," *Journal of Real-Time Image Processing* **18** (2021).
- [12] Liu, J. and Lin, T. H., "A framework for the synthesis of x-ray security inspection images based on generative adversarial networks," *IEEE Access* **11**, 63751–63760 (2023).
- [13] Liu, K., Lyu, S., Shivakumara, P., Blumenstein, M., and Lu, Y., "A new few-shot learning-based model for prohibited objects detection in cluttered baggage x-ray images through edge detection and reverse validation," *IEEE Signal Processing Letters* **30**, 1607–1611 (2023).
- [14] *DSA Detection - TSK6000 Inert Explosives Threat Kit*.
- [15] Takagi, T. and Sugeno, M., "Fuzzy identification of systems and its applications to modeling and control," *IEEE Transactions on Systems, Man, and Cybernetics* **SMC-15**(1), 116–132 (1985).